

Electronic Supplementary Information

Hierarchically Mesoporous Silica Nanoparticles: Extraction, Amino-functionalization and Their Multipurpose Potentials

Xin Du^{1,2}, Junhui He^{1*}

* To whom correspondence should be addressed. Tel.: +86-10-82543535; Fax: +86-10-82543535;

E-mail: jhhe@mail.ipc.ac.cn

- 1. Functional Nanomaterials Laboratory and Key Laboratory of Photochemical Conversion and Optoelectronic Materials, Technical Institute of Physics and Chemistry (TIPC), Chinese Academy of Sciences, Zhongguancun Beiyitiao 2, Haidianqu, Beijing 100190, China*
- 2. Graduate University of Chinese Academy of Sciences, Beijing 100864, China*

Part 1. The calibration curve of ibuprofen (IBU)

The solubility of IBU in pure water at 25 °C is ca. 0.086 mg/mL, but the solubility of IBU in phosphate-buffered saline (PBS, 137 mM NaCl, 2.7 mM KCl, 5.0 mM Na₂HPO₄·12H₂O, 0.7 mM H₃PO₄ in ultrapure water, pH 7.2-7.4) is improved, and is at least 1.5 mg/mL. Four standard solutions of IBU in PBS were prepared, and shown in [Table S1](#).

A calibration curve was obtained by plotting the absorbance of standard solution as a function of the IBU concentration between 0.1 and 1.5 mg mL⁻¹. The calibration curve fits well the Lambert and Beer's law

$$A = 1.6584 C + 0.02439$$

where A is absorbance at 264 nm and C is the IBU concentration (mg mL⁻¹).

Table S1. Standard solutions of IBU in PBS and their UV-vis absorbances at 264 nm

Entry	IBU concentration (mg/mL)	Absorbance
1	0	0
2	0.1	0.191
3	0.5	0.87
4	1	1.721
5	1.5	2.481

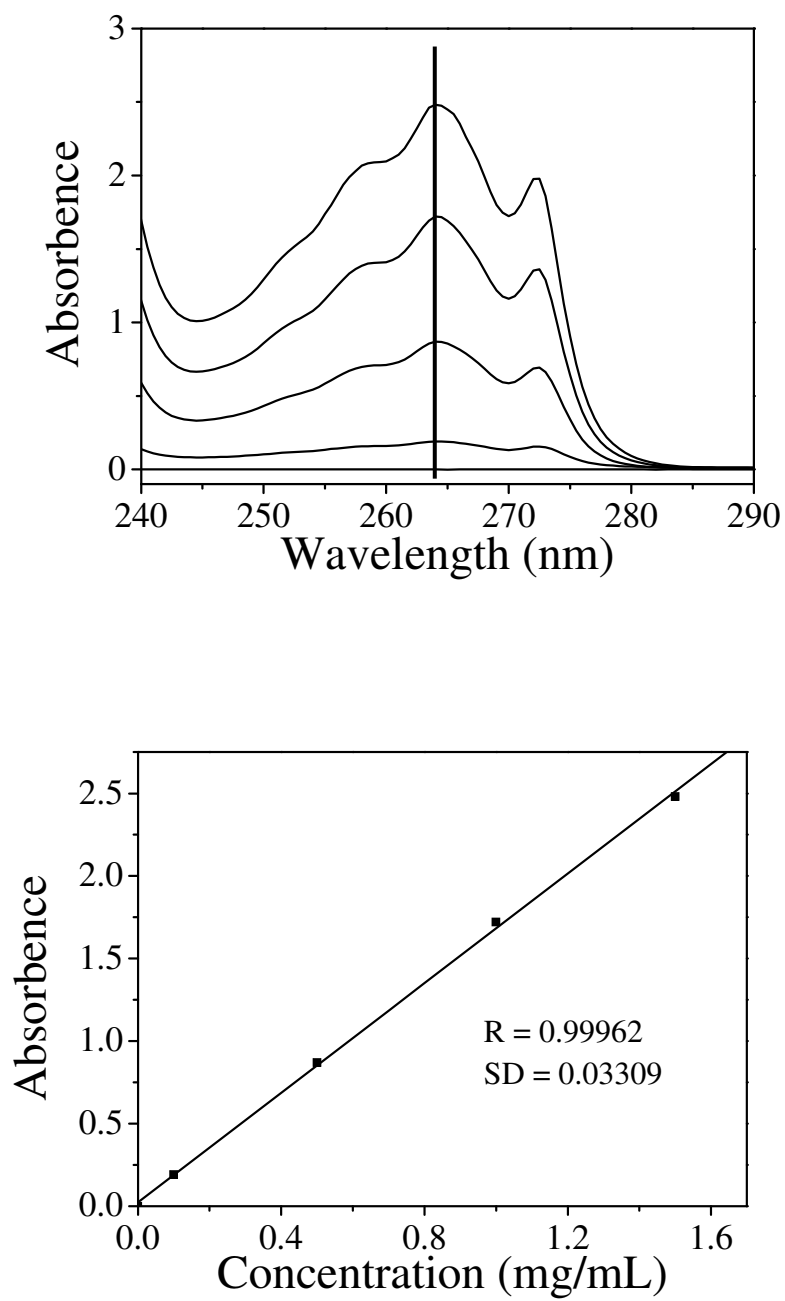


Figure S1. UV-vis spectra of IBU standard solutions in Table S1 and the calibration curve of the UV absorbance at 264 nm vs. the IBU concentration between 0 and 1.5 mg mL⁻¹.

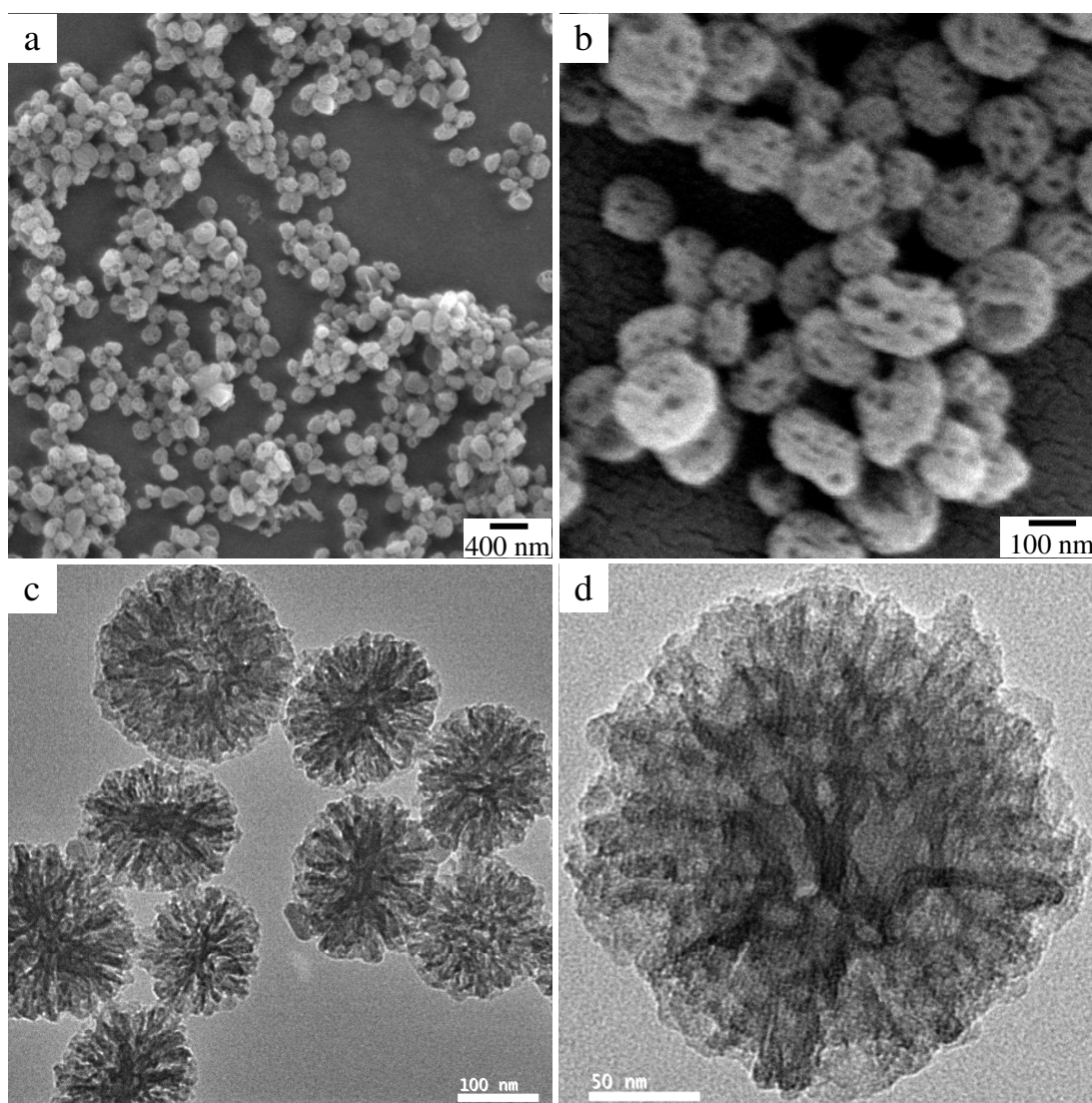


Figure S2. SEM (a,b) and TEM (c,d) images of as-HMSNs.

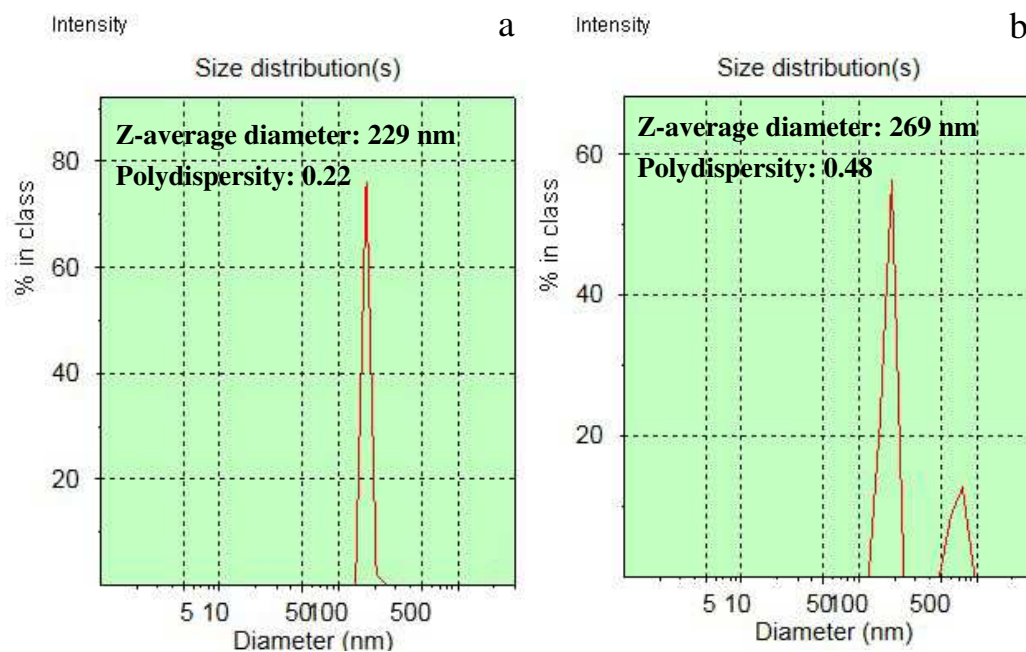


Figure S3. Particle size distributions of ext-HMSNs (a) and NH₂-ext-HMSNs fabricated by post-synthesis modification (b) by DLS measurements. Amino-functionalization results in a slight size increase from 229 to 269 nm and the appearance of a new distribution peak at ca. 600 nm, which indicates that NH₂-ext-HMSNs have a little aggregation.

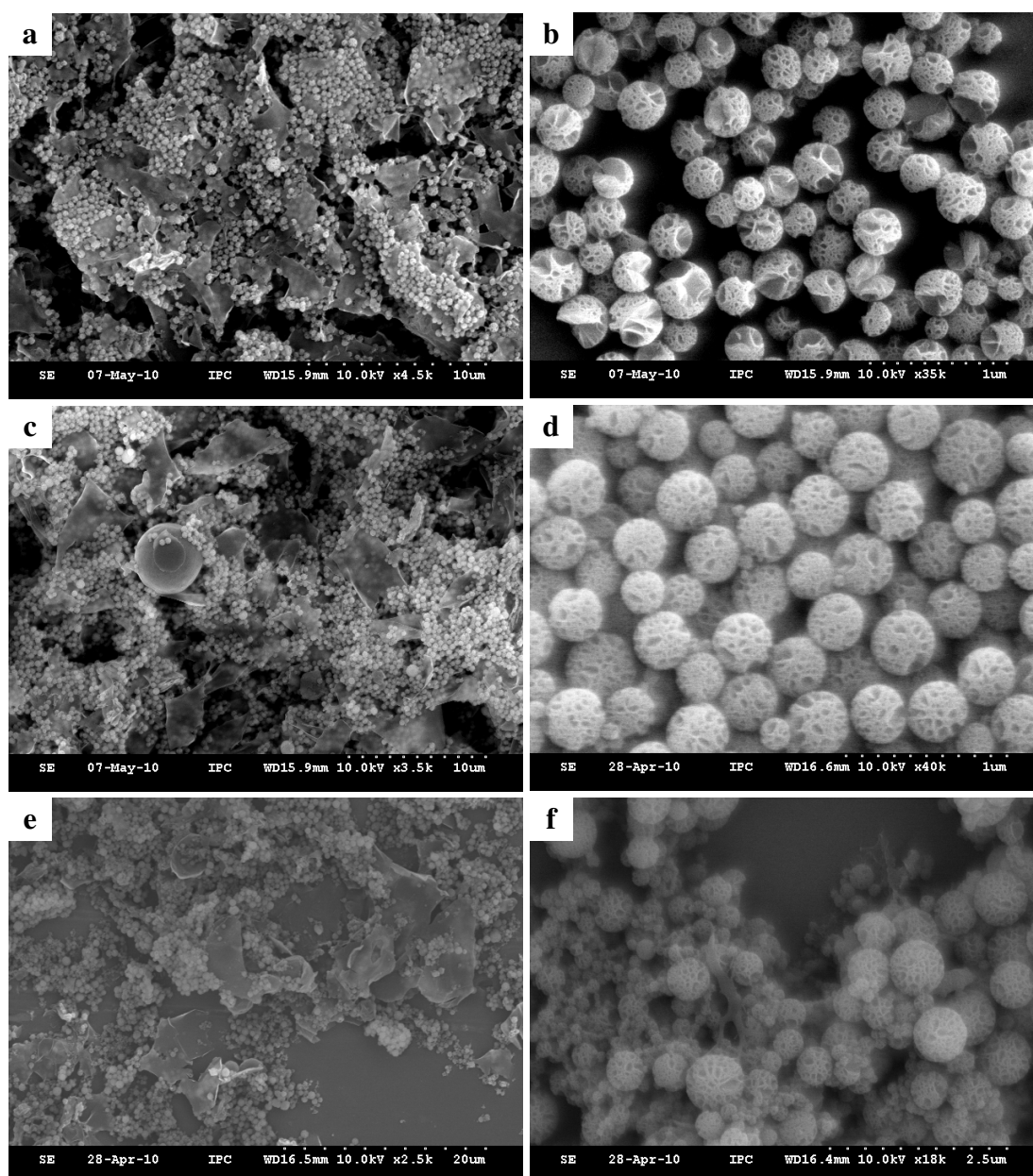


Figure S4. SEM images of products fabricated with addition of varied volumes of APMS as co-condensation precursor: 0.02 (a,b), 0.05 (c,d), and 0.2 mL (e,f).

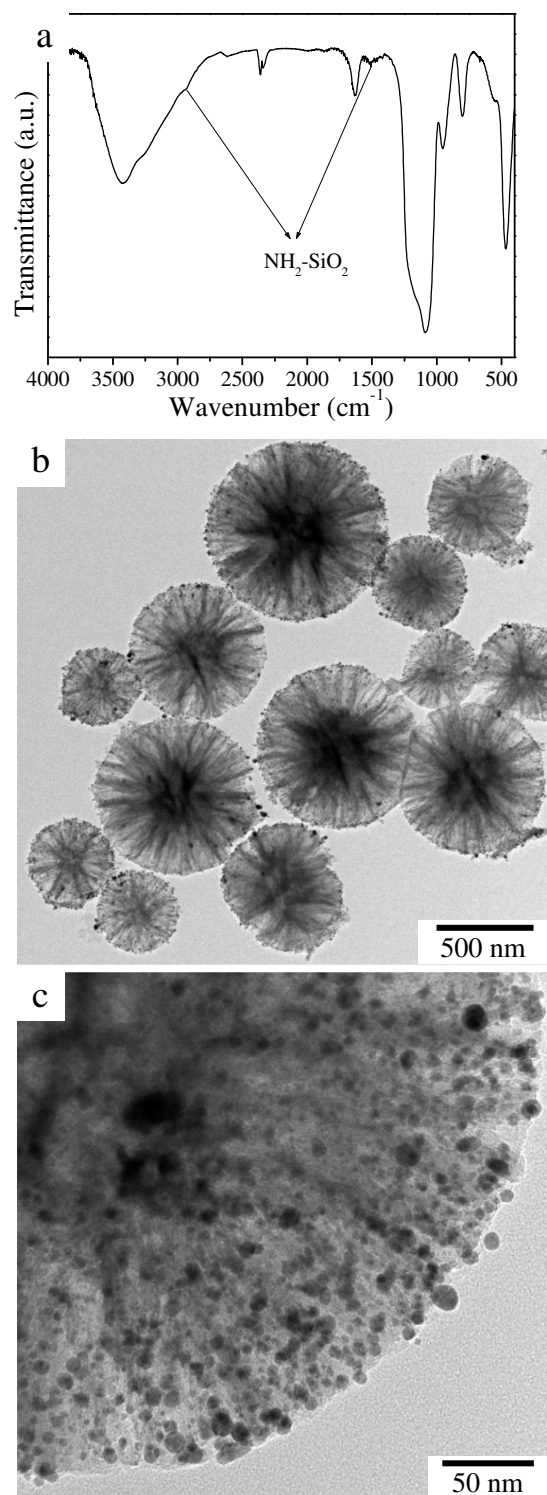


Figure S5. FTIR spectrum (a) of extracted NH_2 -HMSNs fabricated with addition of 0.2 mL of APMS as co-condensation precursor. TEM images (b,c) of the extracted NH_2 -HMSNs after loading with Au nanoparticles according to the process of experimental section.

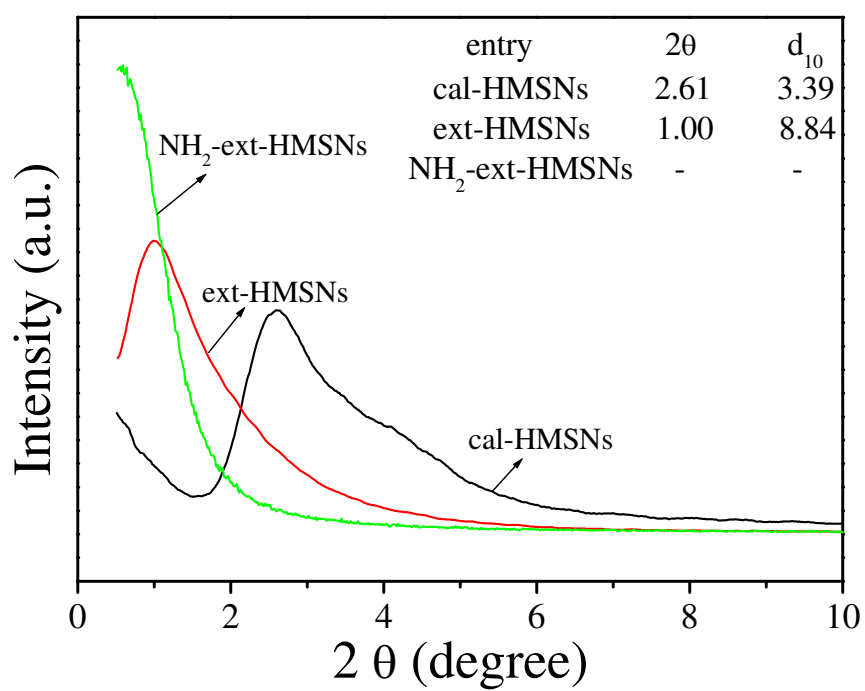


Figure S6 SAXRD patterns of cal-HMSNs, ext-HMSNs and NH₂-ext-HMSNs. The d spacings (d_{10}) were calculated from the XRD peaks of (10) diffraction.

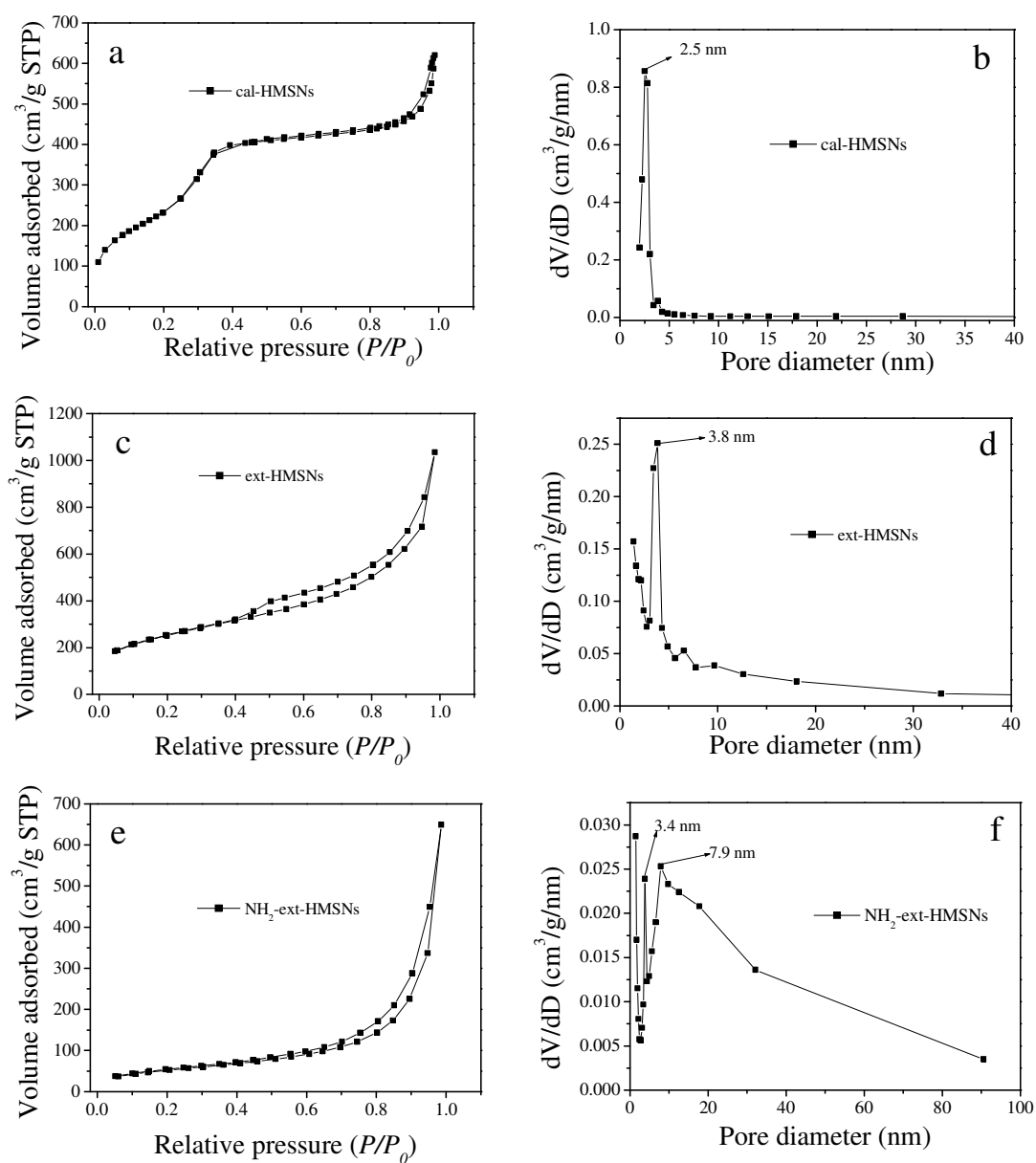


Figure S7 Nitrogen adsorption-desorption isotherms (a,c,e) and corresponding pore size distributions (b,d,f) obtained from desorption branches of cal-HMSNs (a,b), ext-HMSNs (c,d) and NH_2 -ext-HMSNs (e,f).

Table S2 Physicochemical properties of prepared silica structures

Entry	d_{10} (nm) ^a	BET surface area (m ² g ⁻¹) ^b	Pore diameter (nm) ^c	Pore volume (cm ³ g ⁻¹) ^d
cal-HMSNs	3.39	1078	2.5	1.01
ext-HMSNs	8.84	893	3.8	1.60
NH ₂ -ext-HMSNs	-	190	3.4, 7.9	1.01

^a calculated from the SAXRD peak of (10) diffraction.

^b calculated from the N₂ adsorption branch using the BET method.

^c calculated from the N₂ desorption branch using the BJH method.

^d estimated from the single-point amount adsorbed at $P/P_0 = 0.98$.

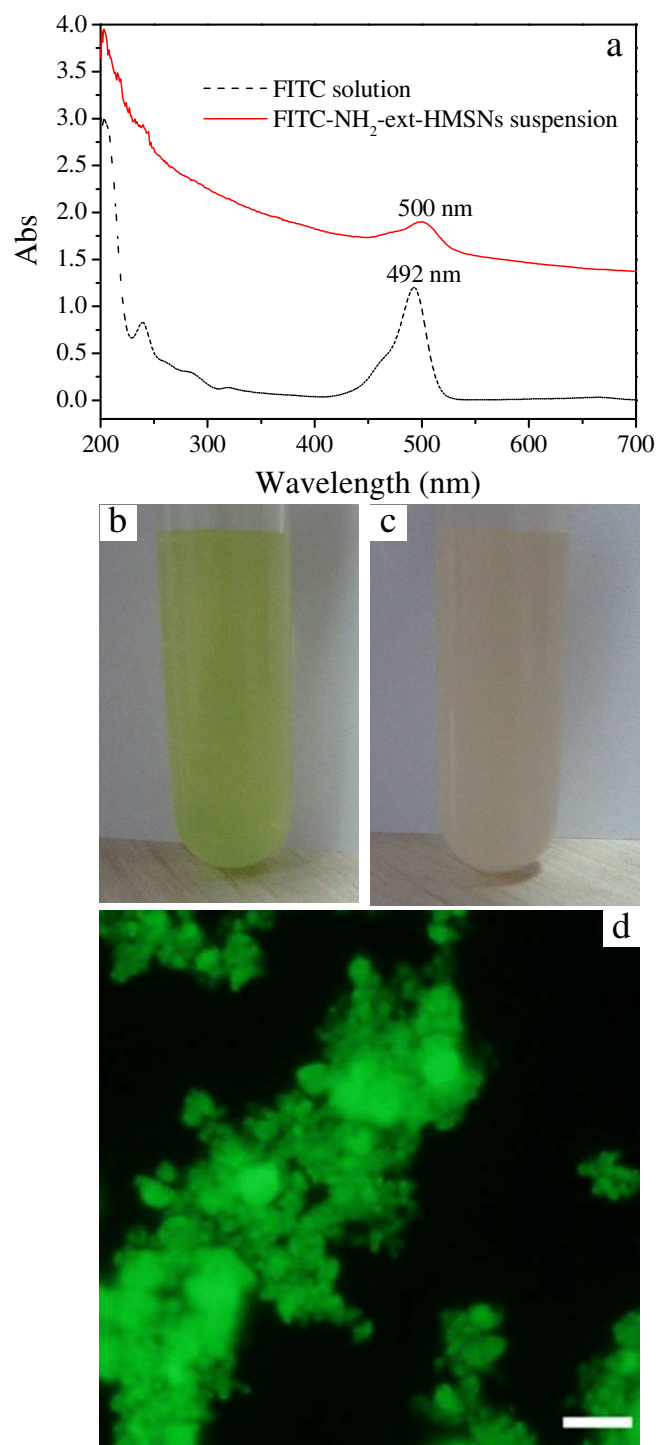


Figure S8. UV-vis absorption spectra (a) of FITC solution and FITC-NH₂-ext-HMSNs suspension, color digital images of FITC solution (b) and FITC-NH₂-ext-HMSNs suspension (c), and confocal microscopy image (d) of FITC-NH₂-ext-HMSNs. The scale bar in (d) is 5 μ m.

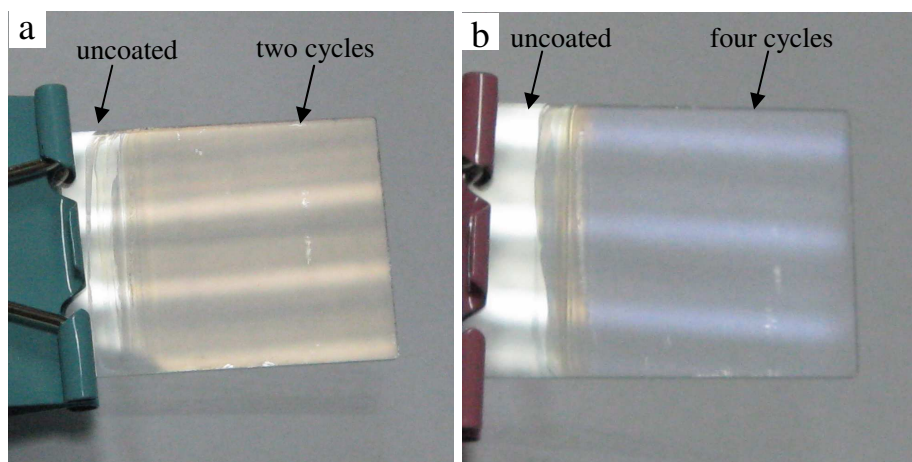


Figure S9. Digital images of slide glasses coated with two (a) and four (b) cycles of PDDA/ext-HMSNs showing the suppression of reflection.

After successful amino-functionalization of ext-HMSNs by post-grafting, NH_2 -ext-HMSNs were dispersed in ultrapure water (ca. 0.5 wt%, pH=8.78) and were also used as building blocks to construct particulate coatings. Protonation of NH_2 -ext-HMSNs results in pH increase from 3.46 (ext-HMSNs) to 8.78 (NH_2 -ext-HMSNs). As NH_2 -ext-HMSNs are positively charged, multilayers of $(\text{PDDA}/\text{PSS})_5$ were prepared, and were used as a primer and the particulate coating of $(\text{PDDA}/\text{PSS})_5(\text{NH}_2\text{-ext-HMSNs}/\text{PSS})_3\text{NH}_2\text{-ext-HMSNs}$ was prepared.

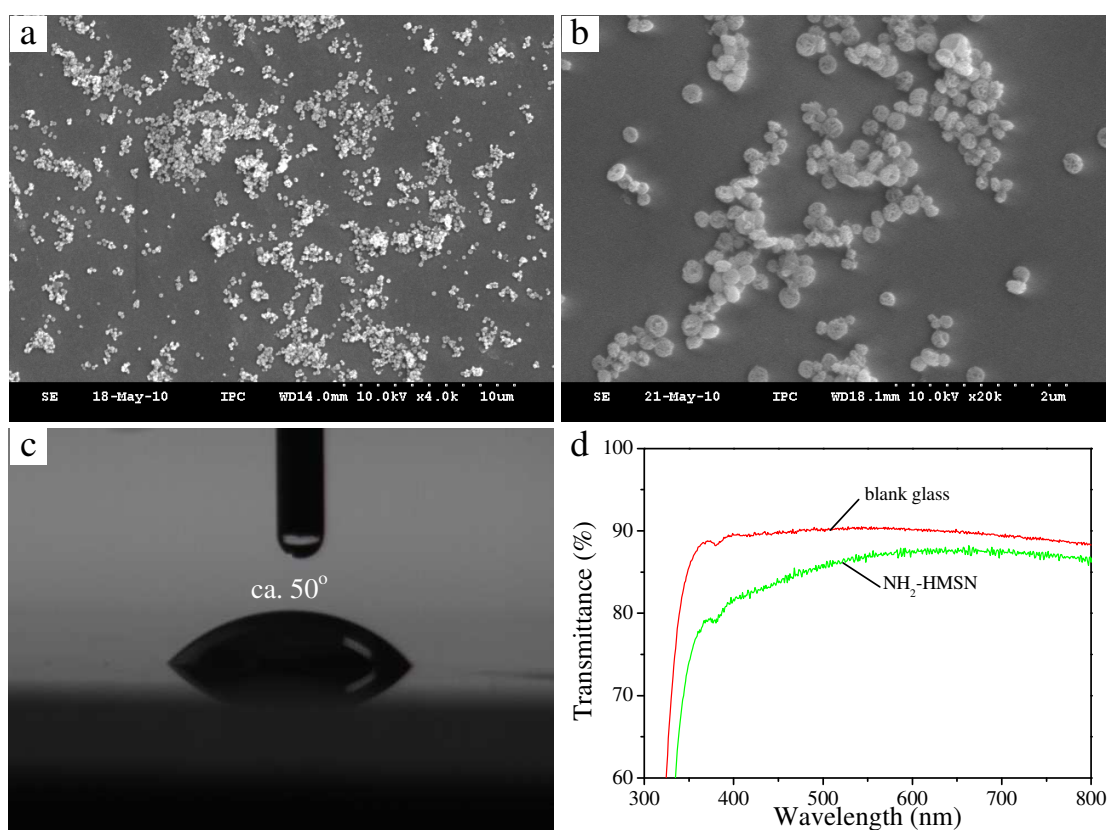


Figure S10. (a,b) SEM images of NH_2 -HMSNs coatings on slide glasses by depositing four cycles of PDDA/NH_2 -HMSNs. (c) Digital image of ca. 50° WCA on the NH_2 -HMSNs coating. (d) Transmission spectra of blank slide glass and slide glass coated with four cycles of PSS/NH_2 -HMSNs.

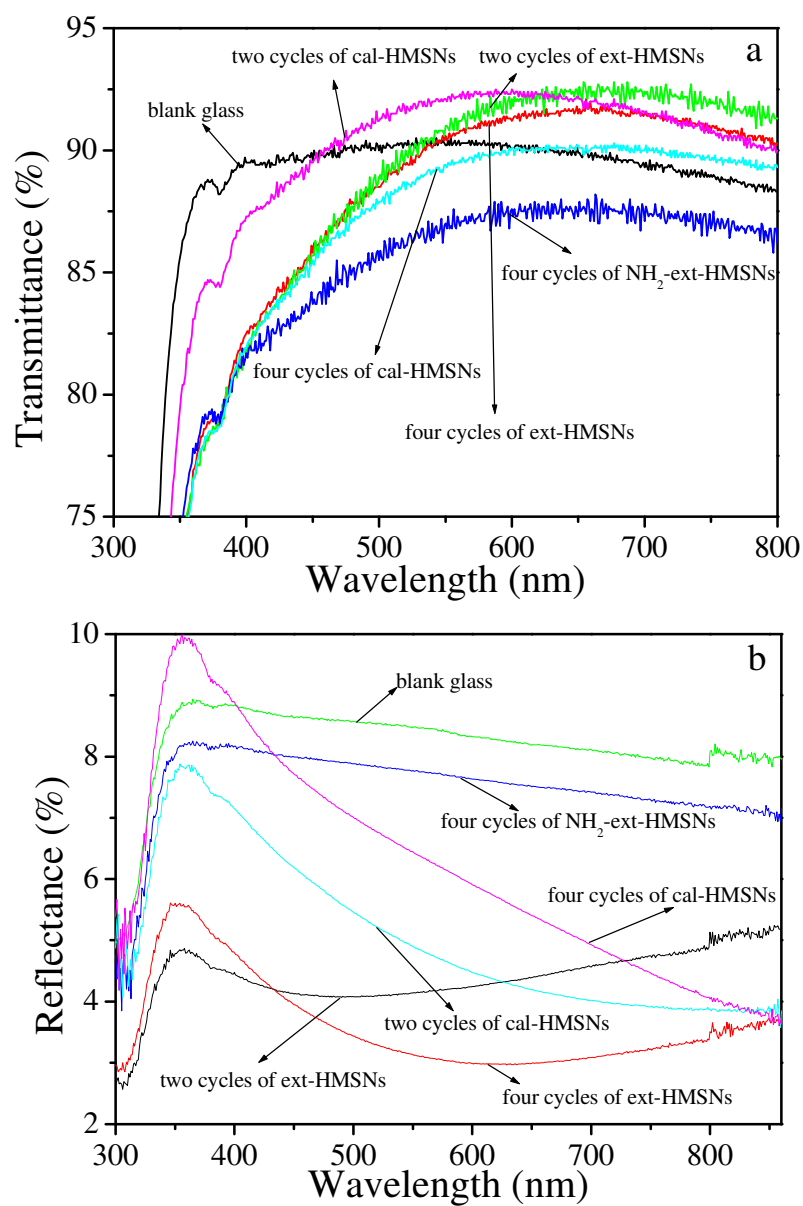


Figure S11. Transmission (a) and reflection (b) spectra of blank slide glass and slide glasses coated with varied particles: ext-HMSNs, cal-HMSNs and NH_2 -ext-HMSNs.